The 5th European sCO_2 Conference for Energy Systems
March 14-16, 2023, Prague, Czech Republic

2023-sCO2.eu-108

SCO2 TEST FACILITY AT TU WIEN: DESIGN, OPERATION AND RESULTS

Viktoria Illyés*
TU Wien
Vienna, Austria
Email: viktoria.illyes@tuwien.ac.at

Stefan Thanheiser
TU Wien
Vienna, Austria

Paul Schwarzmayr
TU Wien
Vienna, Austria

Pierre-Luc David
Kelvion Thermal Solutions
Nantes, France

Xavier Guerif
Kelvion Thermal Solutions
Nantes, France

Andreas Werner
TU Wien
Vienna, Austria

Markus Haider
TU Wien
Vienna, Austria

ABSTRACT

At TU Wien, a test facility working with supercritical carbon dioxide (sCO_2) was commissioned in 2018. Since then, it has been used for various research tasks. This paper gives an overview about the three configurations of the facility with a focus on design, operation, and results.

The authors present the design of components in the three configurations of the test facility: proof of concept of the simple cycle in supercritical and transcritical operation mode, heat transfer measurements, and future work. Special emphasis is given to challenges during engineering and operation. Our most relevant lessons learned are: that a commercial CO_2 pump is not sufficient for cycle experiments, how to design a measurement section for heat transfer measurements, and that during experimental research, measurement-concepts and data reduction must be prioritized at all times.

INTRODUCTION

SCO_2 research progressed since Brun, Friedman and Dennis´ book on sCO2 power cycle activities in 2017, [1]. The chapter "Test facilities", [2], describes four American test facilities in detail and mentions activities in Japan and South Korea. Considering the amount of experimental work in the last years, recent review papers focus on specific topics: Wu et al. [3] focused on Brayton cycles in nuclear engineering applications and White et al. [4] presents sCO_2 turbomachinery designs, most of which are planned to be tested or already were. A list of experimental facilities is given in Table 1. Yu et al.´s bibliometric analysis [5] presents the main players in sCO_2 Brayton cycles: United States, China, South Korea, Australia, and India. This fact more or less also shows in experimental cycles. Europe´s research is clearly not as advanced, having only small scale test facilities and does not execute extensive research in turbomachinery as only two test facilities have a turbine [4]. The TU Wien test facility stands out as it is a transcritical cycle. The review papers show that most of the theoretical and experimental research is done on Brayton cycles with the exception of Net Powers Allam cycle and one of KIER´s cycles being transcritical.

Experimental work with conditions suitable for sCO_2 research is expensive, labor-intensive and full of risks of not having considered every practical aspect. Some of the scientific community acknowledges the need to publish "practical aspects", "guidelines" or "lessons learned". SNL published their lessons learned on the process of constructing and operating the loop for turbocompressor testing [6]. They also provide a guideline of design and operation of sCO_2 R&D systems, [7]. BMPC have published practical aspects of sCO_2 Brayton system testing [8]. In the project report of the Australian solar-driven sCO_2 Brayton cycle, a section is dedicated to lessons learned regarding materials, [9]. Within the sCO2-HeRo project an extensive description of operational experiences is given for the sCO2-HeRo, SCARLETT and SUSEN test loops, [10]. Cranfield University presented broad lessons learned on cost assessment, the test facility and modelling, [11], and on commissioning, [12], and experiments, [13].

In this context, we show never before published results from our facility during its phase of proof-of-concept and early heat transfer measurements. We also include a lessons learned section to give practical advice.

Test facility at TU Wien and its configurations

Three major sets of experiments were conducted or are scheduled in various configurations of the test facility, see Figure 1: testing during the national project, heat transfer measurements and future experiments in the EU-funded project SCARABEUS. In the test facility´s first configuration during our national project, the aim was the proof of concept and gaining experience in operation of the simple transcritical and supercritical cycle.

* corresponding author(s)

DOI: 10.17185/duepublico/77261

Table 1: sCO_2 test facilities, names in italics are brand or project related names.

Organization	Name test facility	Location	Timeframe/status	Ref.	Reviewed
SNL	more than one test rig	Albuquerque, NM, USA	research ongoing with several test rigs	[6], [7]	[2], [3], [4]
SwRI	SwRi SunShot facility, 1 MWe sCO_2 test loop	San Antonio, TX, USA	SunShot finished (2011-2018), last paper published in 2018	[14], [15]	[2], [3], [4]
Echogen Power Systems	*EPS100*	Akron, OH, USA (Olean, NY)	test program in Olean, NY, USA completed in 2014; research ongoing at Akron test facility	[2]	[2], [3], [4]
Naval Nuclear Laboratory op. by BMPC	*Integrated System Test (IST)*	West Mifflin, PA, USA	finished	[8]	[2], [4]
GTI Energy, SwRI, GE Global Research, DOE many others through Joint Industry Program	*STEP Demo*, 10 MWe sCO_2 Pilot Plant Test Facility	San Antonio, TX, USA	commissioning and start-up expected late 22 or early 23, testing in 23	[16]–[18]	[3]
Net Power, Baker Hughes	*50-MWth test facility, Serial #1 Utility Scale Plant*	La Porte, TX, USA	La Porte demonstration site connected the grid in fall 21 (2012-2021), first utility-scale power plant in Permian West, TX expected to go online in 26	[19], [20]	[4]
KAERI, KAIST, POSTECH	*SCIEL*	Daejeon, KR	finished	[21]	[2], [3], [4]
KAIST, KAERI	*SCO2PE*	Daejeon, KR	finished	[22], [23]	[2]
KIER	5 cycles so far	Daejeon, KR	full 5th cylce commissioning expected in 2020, not yet published	[24], [25]	[2], [3], [4]
TIT, IAE	bench scale test facility	Tokyo, JP	finished	[26]	[4]
Shouhang, EDF	10MWe supercritical cycle + CSP demonstration	Shouhang, CN	2018-2023, commissioning of retrofit cycle to industrial CSP plant planned end of 2021, no news since end of 2019	[27]	[4]
CHNG, TPRI	5 MW fossil-fired supercritical CO_2 power cycle pilot loop	Xi´an, CN	experiments were planned in 2020, no news since19	[28]	[3]
Indian Institute of Science, SNL	test facility for supercritical CO_2 Brayton cycle	Bangalore, IN	research seems ongoing	[29]	/
CSIRO	Solar-Driven Supercritical Brayton Cycle	Newcastle, AUS	project completed (2012-2017), now collaboration with US DOE => joined the STEP Demo project	[9]	[3]
The University of Queensland	Refrigerant and Supercritical CO_2 Test Loop, *PHPL*	Queensland, AUS	no news on test loop since 2016; ASTRI project ongoing, demonstration planned end of 22	[30]–[32]	/
Baker Hughes	Prototype compressor test rig	Florence, IT	2018-2021, results paper published in 2022	[33]	/
CVR	*SUSEN* test loop	Prague, CZ	since ~2007, research on several experimental projects (e.g., COMPASsCO2) is ongoing	[34], [35]	/
IKE	*SCARLETT*	Stuttgart, DE	finished, team involved in other sCO_2 projects	[36], [37]	/

DOI: 10.17185/duepublico/77261

Table 1 continued					
Organization	**Name test facility**	**Location**	**Timeframe/status**	**Ref.**	**Reviewed**
Project Consortium (University Duisburg-Essen, CVR, University of Stuttgart)	*sCO2-HeRo* loop	Duisburg, DE	projects sCO2-HeRo (2015-2018), sCO2-Flex (2018-2021) and sCO2-4-NPP (2019-2022) finished	[10], [38]	[4]
Cranfield University	*Rolls-Royce sCO2 Test Rig*	Bedfordshire, UK	research ongoing, in operation	[11]–[13]	/
Brunel University, Engoia	*HT2C* facility	London, UK	project I-ThERM finished (2015-2021)	[39]	[4]
LUT University	*LUTsCO2* facility	Lappeenranta, FIN	only design published so far, research ongoing	[40]	/
TU Wien	sCO2 test facility	Vienna, AUT	project SCARABEUS (2019-2023) ongoing, experiments expected in 23	This paper.	/

The experimental set-up consisted of the pump, a heater, an expansion valve as a substitute for the turbine, a water-cooler and a tank, see Figure 2. The CO_2 was heated up to 320 °C with thermal oil and reached a pressure of 240 bar at a mass flow rate up to 0.33 kg/s.

In the second configuration, heat transfer measurements were conducted for heating up supercritical CO_2 at pressures up to 220 bar and temperatures up to 150 °C. For cooling and condensing experiments, the test facility was modified with a new test section including a precooler and test tubes with microfins and several improvements were undertaken. The experiments took place at sub- and supercritical pressures up to 100 bar, temperatures up to 180 °C and for a working fluid consisting of pure CO_2 and a CO_2+refrigerant mixture.

In the third configuration (SCARABEUS), the test facility operates as a recuperated Rankine cycle. The commissioning will take place in April 2023. The facility will operate at high temperatures up to 650 °C. One part of the planned research focuses on Printed Circuit Heat Exchangers (PCHE): two different designs will be tested. The main focus, however, lies on testing novel zeotropic CO_2-based working fluids that allow condensation at high temperatures. The goal is to condense the working fluid at air temperatures as high as 35 °C, which we will prove by experiments.

NATIONAL PROJECT	HEAT TRANSFER	SCARABEUS
• Simple cycle layout with expansion valve • Tmax=320 °C • Pmax=240 bar	• Test section for heat transfer when heating up supercritical CO_2 • New test section for cooling & condensing • Several improvements in cycle	• Recuperated cycle • Tmax= 650°C • Pmax=235 bar • Air cooled condenser • Printed circuit heat exchangers as recuperator
• Proof of concept and practical knowledge of transcritical and supercritical cycle	• Heat transfer measurements • Pure CO_2 • CO_2 + refrigerant mixture	• Proof of concept of CO_2 mixtures (at high temperatures and condensing with ambient air)

Figure 1: visualization of projects and tasks.

The paper is structured in four parts: 1) a design section covering the national project, heat transfer, and SCARABEUS, 2) a section about operation and results of the national project, 3) methods and results of the heat transfer measurements, and 4) a selection of our lessons learned.

DESIGN – NATIONAL

The test facility in its first configuration consists of five major parts, as can be seen in Figure 2 and Table 2. The high- and low-pressure sides are designed for pressures up to 240 bar and the 100 bar, respectively. The piston pump is able to provide a mass flow rate of up to 0.33 kg/s and can move liquid and supercritical CO_2 under some constraints. The CO_2 is heated up to 320 °C in a 200 kW shell-and-tube heat exchanger with the thermal oil Therminol VP-1. An expansion valve substitutes the turbine´s pressure loss. The cooler is a shell-and-tube heat exchanger with water as a coolant. During start-up and in transcritical mode, the CO_2 is present in liquid form and stored in the tank. In supercritical mode, the tank is by-passed.

In this configuration, operation of the transcritical and supercritical cycle was tested. The conditions during experiments are shown in Figure 3. The pump receives the CO_2 from the tank, where it is liquid in the case of the transcritical operation. With a cooling water temperature of around 8 °C, working fluid temperatures as low as 15 °C corresponding to a pressure of ~43 bar can be achieved at state 1. The upper limit for transcritical operation is 26 °C to have a sufficient margin to the critical point. In Figure 3, a temperature of 19.5 °C and a corresponding pressure of 56.6 bar on the low-pressure side is shown. At the outlet of the piston pump, state 2, while cooling the pump with water, the outlet temperature is at around 40 °C. The CO_2 then enters the heater and reaches a temperature of up to 320 °C for which the inlet thermal oil temperature is at 360 °C. The expansion valve mimics the pressure loss of the turbine and is controlled to set the high pressure of the system to 220 bar. After expansion, the still hot CO_2 at the system´s low-pressure side enters the water cooler, which controls the temperature (and thereby the pressure) at state 1. For supercritical operation, the facility is started up in transcritical operation. Then, the tank is

DOI: 10.17185/duepublico/77261

bypassed by cutting it off with automatic valves. The cooler slowly increases the temperature until the pressure on the low-pressure side reaches supercritical values at 4* and 1*. States as shown in Figure 3, yellow colored isobaric line, could not be reached with this approach because the facility does not have a mass management system for the working fluid.

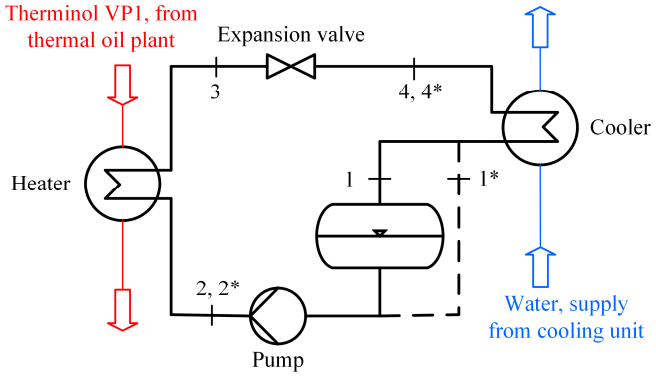

Figure 2: scheme of major components of the test facility.

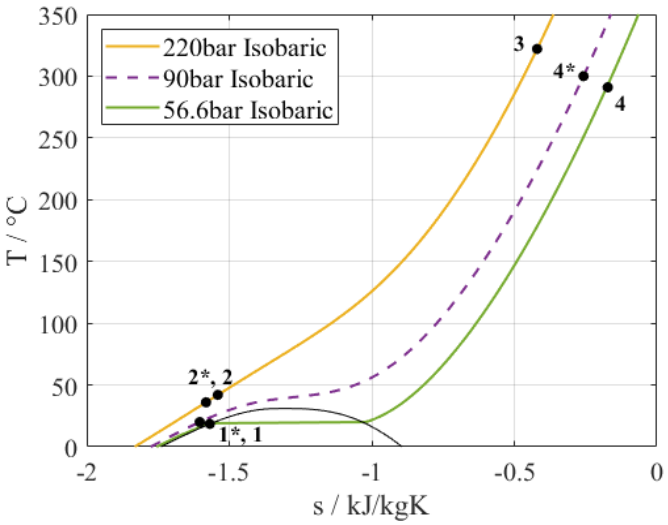

Figure 3: Ts-diagram of supercritical and transcritical cycle conditions as tested in the facility.

Table 2: List of major components of the test facility.

Component	
Heater	200 kW, Shell-and-Tube, CO_2 tube-side, thermal oil VP-1 shell-side
Cooler/ condenser	355 kW, Shell-and-Tube, CO_2 tube-side, water shell-side
Pump	Piston-pump (SPECK-TRIPLEX-PLUNGERPUMPE P52/51-300CZ), max. 50 L/min, P_{max}=280 bar
Expansion valve	Pneumatic control valve, type 3252
Tank	55 L

For heat input, an electrically heated thermal oil is used. It is provided by an external utility. Although Therminol VP-1 can be used for temperatures up to 400 °C, the maximum inlet temperature in the primary heat exchanger of the CO_2 facility is limited to 360 °C as the thermal oil has to be pressurized to prevent evaporization at these high temperatures. The systems pressure needs to be at around 10 bar.

For the working fluid we use CO_2 of food grade, by Linde under the name Biogon C E 290. It has a quality of more than 99.7 % CO_2. We buy gas cylinders with riser pipe to be able to fill the test facility with liquid CO_2. It has to be assumed that the CO_2 gets contaminated with lubricant from the pump as this was observed during plant modification.

For safety, a Hazard and Operability Study (HAZOP) under professional lead was performed after the functional design of the plant. A hard-wired shut-down of safety and integrity level 2 (SIL2) of the thermal oil pump and heater in the case of excessive temperature was necessary. The number and position of safety valves was determined. For heat exchangers, it is necessary to consider a rupture of a heat exchanger pipe. In this case, the CO_2 from the high-pressure side of the heat exchanger would expand towards the low-pressure-shell-side, which is designed for 16 bar. The water line's design pressure is only 8 bar. The expanding CO_2 from the test facility's high-pressure levels into the low-pressure heating and cooling systems would lead to overpressure there. As the CO_2 would mix with water (cooler) or thermal oil (heater), the amount of gas-liquid-mixture to be discharged would have been too high to deal with for a safety valve. The solution was to include burst discs directly on the heat exchangers´ low-pressure side. A system of flash lines and flash tanks were designed to collect the blown out mixture. All the parts of the test rig were pressure tested individually with water. A leak test under supervision from the notified body was performed with nitrogen in the finished version of the facility as a last step before approval. After that, major modifications have to be checked and approved by the notified body.

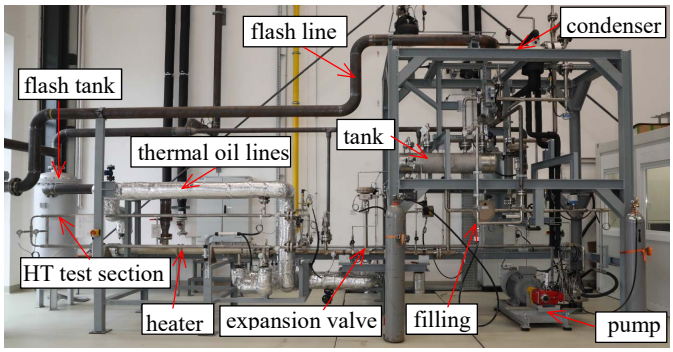

Figure 4: components of the test facility.

DESIGN – HEAT TRANSFER

First test section

The first test section for measuring the heat transfer coefficient of CO_2 to the inside of a tube wall is depicted in Figure 5. The

DOI: 10.17185/duepublico/77261

test section, a counter flow heat exchanger, consisted of a single tube with the CO_2 flowing inside, surrounded by an outside shell where thermal oil (VP-1) provided the heat source. The tube was U-shaped, where each U-part was about 3 m long. Regrettably, the design suffered from a lack of time and money. The results were not as expected and practically unusable due to the following issues:

- The Coriolis sensor that measured the mass flow of CO_2 into the test section was positioned upstream on the low-pressure side of the pump. This meant that the (by-design) leakage across the high-pressure gaskets inside the pump could not be accounted for during the heat transfer measurements upstream.
- Since the flow of CO_2 from the tank to the pump was in a saturated state, any heat from the environment transferred to the working fluid cased evaporation, leading to a two-phase flow in the Coriolis sensor and further degrading its accuracy. Density measurements that were also available from the Coriolis sensor could have at least indicated a two-phase flow, but they were not recorded during that early tests (yet).
- The test section had practically no straight inlet section that could have normalized the CO_2's flow profile, causing heavy turbulences in the first section.
- The bend in the middle of the test section is simply impractical and should have been avoided. A straight tube would have been easier to handle concerning all aspects of heat transfer measurements and result analysis.
- If a bend was necessary, it should have been in a horizontal rather than a vertical plane. The hydrostatic pressure difference between the U-parts already complicates the measurements.
- The entire measurement concept was not thought out well. Instead of measuring surface temperatures, only bulk inlet and outlet temperatures were measured. This meant that further assumptions on the heat transfer mechanism, in particular on the thermal-oil side, had to be made, decreasing the accuracy of the final results. Additionally, some of the boundary conditions for typical heat transfer correlations were not met.
- The special behavior of CO_2 near the critical point was not considered at all. Non-equilibrium effects greatly influence the heat transfer under such conditions. Non-equilibrium is due to thermo-physical properties barely reaching a stationary state. For example, the density experiences a hysteresis effect depending on the direction of the isobaric process it is undergoing [41].
- The sensors used were of poor quality, resulting in high inaccuracies. The PT100 resistance temperature detectors (RTDs) were 3-wire and only class B.
- Even though the greatest impacts on heat transfer are expected to occur at pressures slightly above the critical pressure (going through the pseudo-critical point), and only coolers would be operating at such pressures in a supercritical CO_2 power cycle, the test section could only be used to measure the heat transfer coefficient when heating the CO_2.

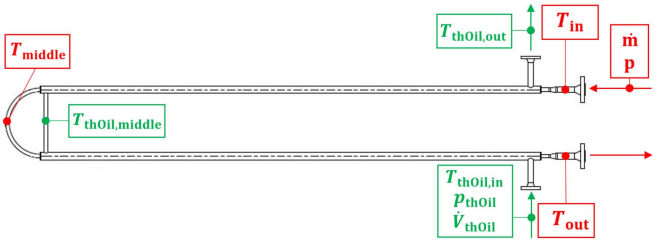

Figure 5: First test section for heat transfer measurements of pure CO_2.

Second heat transfer test section: precooler, test tubes

During our current project SCARABEUS, the facility was extended by a new test section to measure the heat transfer during in-tube cooling and condensation under enhanced heat transfer conditions by using microfins on the inner surface. This new test section is a horizontal tube-in-tube heat exchanger cooled by water. The positions of measurement devices are shown in Figure 6 and Figure 7. To control the inlet vapor content of CO_2, a precooler was installed.

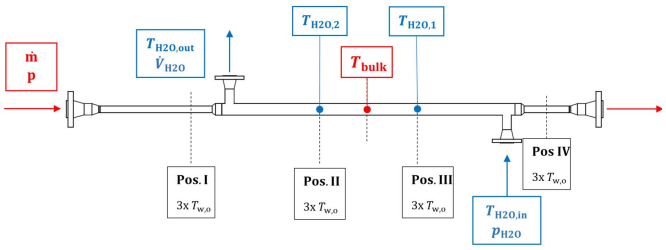

Figure 6: schematic of current test tube for heat transfer measurements when cooling and condensing; red…working fluid, blue…water, black…wall temperature.

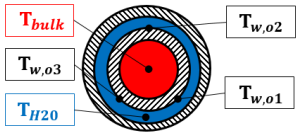

Figure 7: position of the temperature sensors at the cross section of the current test tube.

Many of the first test section´s flaws were eliminated. The most important being (many) high level temperature sensors (PT100, 4-wire, class AA). These were located directly in the CO_2, in the water channel and at the outer wall of the inner tube.

A much lower uncertainty of reduced data can be observed in this new heat transfer measurement section. A part of those experiments is shown in [42].

DESIGN – SCARABEUS

The SCARABEUS concept (Supercritical CARbon dioxide /Alternative Blends for Efficiency Upgrade of Solar power plants) envisions a power block to be coupled with concentrated solar power (CSP) plants. Using a CO_2-based, binary mixture as a working fluid instead of water/steam, this cycle shows an improved efficiency, smaller turbomachinery, fewer equipment

DOI: 10.17185/duepublico/77261

and an air-cooled condenser that enables dry cooling. Even at high ambient temperatures, condensation of the working fluid becomes feasible with ambient air, thus, making a recuperated Rankine cycle possible. The change in properties necessary to enable condensation with air at high ambient temperature is achieved by blending the CO_2 with an additive with a higher critical point. Condensation of a mixture undergoes a temperature glide as the isobaric lines in the two phase region are sloped in the T,s-diagram, see Figure 9. Therefore, condensation of binary mixtures shows less irreversibilities compared to condensing a pure fluid.

The test facility is used for the experimental validation of the SCARABEUS concept in a slightly changed layout as can be seen in Figure 8 and will test one mixture as a working fluid. As of today, a carbon dioxide and hexafluorobenzene (C_6F_6) mixture of 8 % molar fraction of C_6F_6 will be used. The mixture did not perfectly meet all target properties but presents the best compromise. It is thermally stable up to 600 °C [43], slightly toxic (same hazard class as CO_2) and moderately flammable. To reduce the operational risks, a lower percentage of C_6F_6 will be used than we would suggest for an actual plant. The target maximum temperature of 650 °C had to be reduced to 550 °C.

For the chosen mixture, the T,s-diagram looks as shown in Figure 9. The Peng-Robinson EoS with a binary interaction parameter of k_{ij}=0.033 was used to calculate the properties. This approach shows good agreement with experimental data of compositions close to design (around 85% molar fraction of C_6F_6). The critical point is estimated at around 70 °C and 107 bar. Thermo-physical properties at and near the critical point cannot reliably be calculated by EoS as these usually have convergence issues and give no solutions at these conditions.

Compared to pure CO_2, the two-phase region reaches higher temperatures and isobaric lines are sloped in the two-phase region of the T,s-diagram. This means that condensation of the mixture happens in a temperature glide. For example, at a low pressure of 95 bar, the working fluid would start condensing at 106 °C and be fully liquid at around 52 °C.

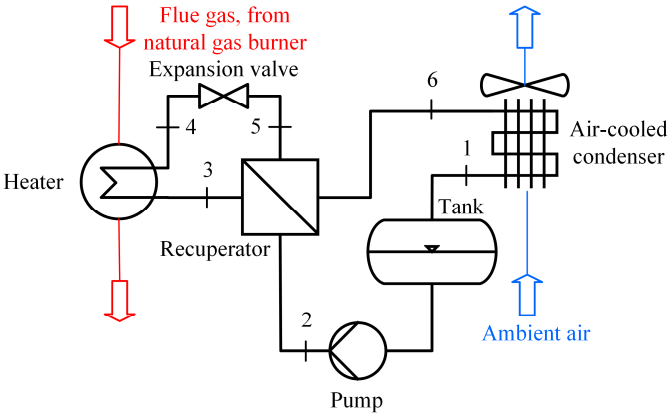

Figure 8: scheme of major components of the test facility as for the SCARABEUS project.

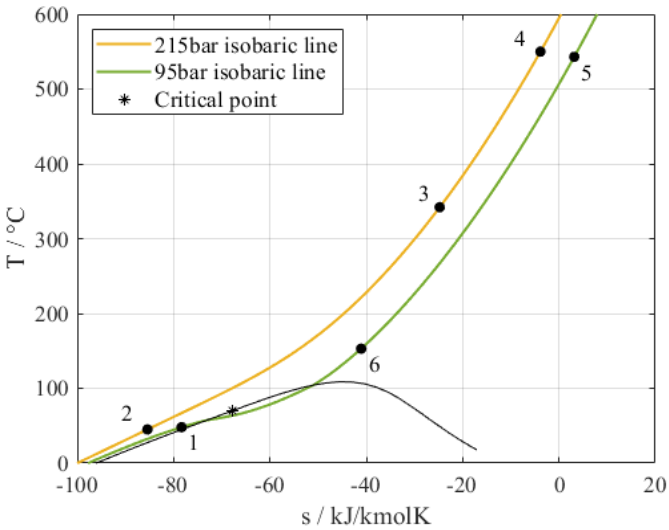

Figure 9: T,s-diagram with recuperated cycle states as to be tested in the facility operated with CO_2+C_6F_6.

Three new heat exchangers make up the modified cycle, each of them specifically designed for the CO_2+C_6F_6 mixture, but for 650 °C since at this time we did not know about temperature limitations due to thermal degradation:

Table 3: list of components for SCARABEUS.

Component	
Heater	220 kW, supplies the cycle with a design temperature of 650 °C by using 850 °C flue gas from a natural gas burner, material: Inconel 617
Air-cooled condenser (ACC)	120 kW, fins at the air-side and microfins at the inner surface, for heat transfer enhancement see [42] and [44]
Recuperator	350 kW, Printed circuit heat exchanger (PCHE), stainless steel
Expansion valve	Custom-built valve to withstand 650 °C

The recuperator – a printed circuit heat exchanger

The recuperator will be a printed circuit heat exchanger (PCHE), a technology of compact heat exchangers withstanding high pressures and temperatures while ensuring high safety levels. Two PCHE´s with different geometries will be tested: airfoil and S-shaped.

To determine optimized geometries, a CFD analysis was carried out with ANSYS CFX 2019 R3. Besides proper boundary conditions representing the thermal-hydraulic problem at hand, the mesh and the chosen turbulence model have the biggest impact on the results of the simulation. Therefore, a mesh independency study was conducted to be able to get reliable results as well as the best possible ratio of good results to simulation time. The selection of a fitting turbulence model can't be handled separately because the quality of the mesh directly influences the results with the chosen turbulence model. Vice versa, there are different requirements on the mesh for different turbulence models. In the used software package, many different

DOI: 10.17185/duepublico/77261

models are available. The refinement of the boundary layer, the overall refinement of the mesh as well as the number of elements around the fins with particular attention to the fillets at the beginning and the end of the fins were modified. Based on experimental results from a zig-zag configuration heat exchanger for H_2, from two turbulence models k-ε and SST, SST was chosen as it better predicts the pressure losses.

Temperature prediction was equally good for both models. Figure 10 shows the geometrical model of the airfoils, the characteristic dimensionless numbers and the channel modelled in CFD. Figure 11 shows the S-shape. As mechanical stress peaks would occur at the sharp edge of the airfoil, it is slightly rounded which is in line with the manufacturing requirements. The trivial result of maximizing the heat transfer rate to pressure drop ratio leads to large numbers for the horizontal and vertical pitch and therefor to bigger overall dimensions of the PCHE. Bigger dimensions generally mean higher material and manufacturing costs. Instead, the optimization is fed with a zigzag channel PCHE as a reference case and the surface area is reduced by the optimizing function at a given heat transfer and pressure drop.

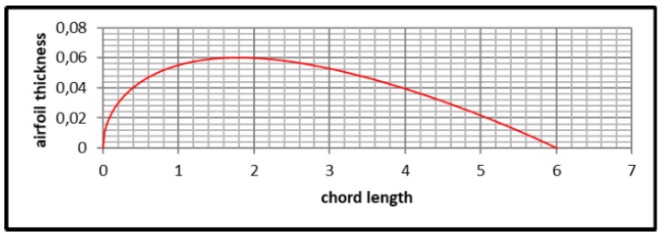

$$y(x) = \frac{L_T}{0{,}2}\left(0{,}2969\sqrt{\frac{x}{L_C}} - 0{,}126\left(\frac{x}{L_C}\right) - 0{,}3537\left(\frac{x}{L_C}\right)^2 + 0{,}2843\left(\frac{x}{L_C}\right)^3 - 0{,}1015\left(\frac{x}{L_C}\right)^4\right)$$

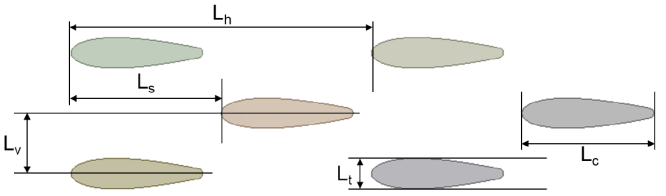

Dimensionless number	Definition
Staggered	$\zeta_S = 2L_s/L_h$
Horizontal	$\zeta_H = L_h/L_C$
Vertical	$\zeta_V = L_v/L_t$

Figure 10: Geometrical characterization and modelling in CFD of airfoil shape.

The CFD results show that S-shape configuration with lower vertical pitches and airfoils in almost every parameter set show a reduction in surface area when compared to zigzag channels.

The following design conclusions can be made about the S-shape:

- Transverse pitch ↑ means size reduction ↓
- Vertical pitches ↓ means performance ↑
- Further decreasing the pitch is not possible due to manufacturing.
- A maximum of 7.6 % of surface reduction is possible with S-shapes compared to zigzag.

For airfoil, the following is true:

- No clear dependencies on parameters
- Staggered number ↑ means size reduction ↑ (So, staggered arrangement performs best while inline arrangement performs worst.)
- Effects of vertical and horizontal number are correlated, see Figure 12
- With a Multi-Objective Genetic Algorithm, the optimized airfoil shape leads to a surface reduction of 17.7 % compared to the zigzag shape.

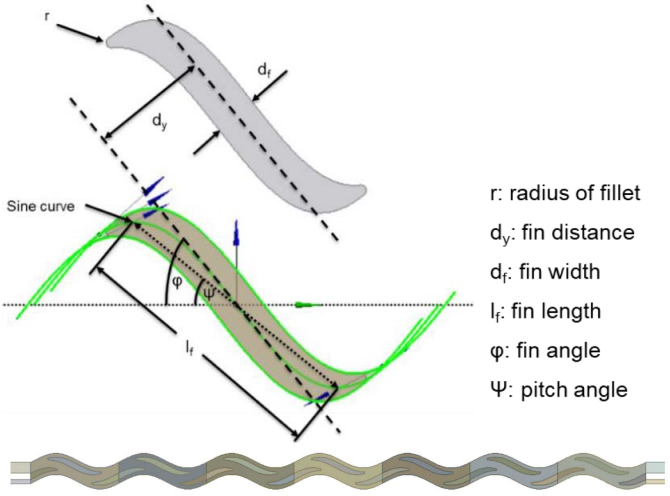

Figure 11: Geometrical characterization and modelling in CFD of S-shape.

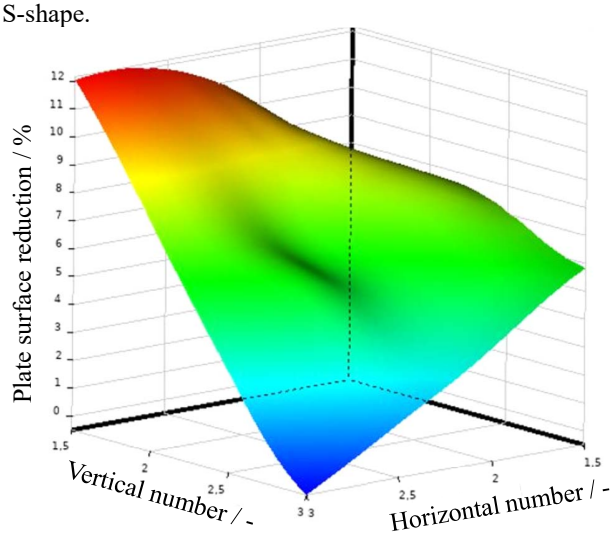

Figure 12: Correlation between vertical, horizontal number and surface reduction at a staggered number of 0.5.

DOI: 10.17185/duepublico/77261

Safety

Additional safety measures are necessary when working with hazardous substances in relevant amounts in an indoor test facility. A fire-resistant enclosure surrounds the entire test facility, see Figure 13 and Figure 14. It serves two purposes: 1) closing off the air supply in the case of fire and preventing the spread of fire for thirty minutes and 2) providing a space for continuous air ventilation during normal operation to dilute potential leakage and venting it outside over the chimney.

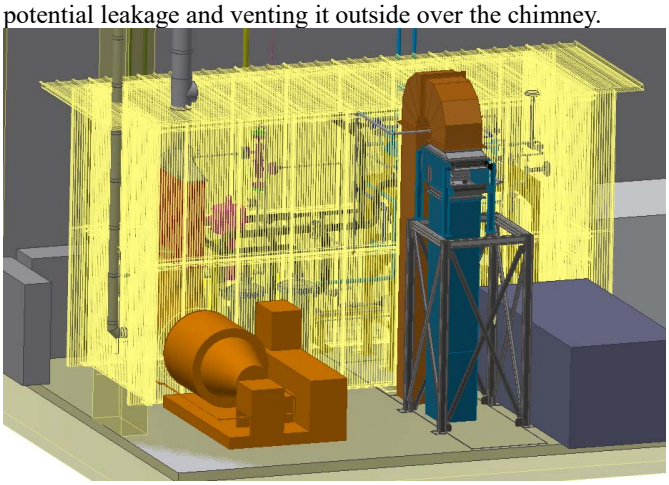

Figure 13: fire-resistant enclosure as planned.

Figure 14: fire-resistant enclosure steelframe as built.

Breaking new ground in research, e.g., adding a hazardous substance to your working fluid and heating it up to 650 °C, can be challenging when it comes to questions of safety.

The first issue is thermal degradation of substances at this elevated temperatures. Small scale testing was accounted for in the project plan of SCARABEUS and showed the limits for operation in the test facility. No laboratory would give a quote on identifying the degradation products which made it impossible to test the 650 °C and potentially create lighter harmful substances with the fluoride from C_6F_6.

The second issue is flammability, which is the case for hexafluorobenzene. Since the substance is rarely used, no data on flammability in the mixture with carbon dioxide diluted in air at extreme conditions (leaking from 220 bar and 650 °C to ambient conditions) is available.

The third issue is toxicity and reactivity. Carbon dioxide itself is hazardous to humans as it is an asphyxiant gas. Three CO_2 detectors at the vicinity of the test facility are used to detect potential leakages in the range of allowed workplace concentrations. Small leakages of the CO_2+C_6F_6 mixture do not bring an additional risk with them since the enclosure contains those possible leakages and C_6F_6 will condensate at ambient conditions. From theoretical analysis, sulfur dioxide (SO_2) and titanium tetrachloride ($TiCl_4$) might seem a good additive choice for SCARABEUS, but SO_2 is highly toxic and $TiCl_4$ is reactive with air humidity and releases hydrochloric acid.

For a test facility of our size and relevant mixtures defined by the project, one filling with SO_2+CO_2 would involve 40 kg of SO_2. When a burst disc breaks, this amount would be released to the surroundings. During the proposal, the idea was to pass the released amount over an active carbon filter to strip the additive. SO_2 can only be stripped if active carbon is impregnated with potassium carbonate and its efficiency is decreased at elevated temperatures, even at 50 °C. There is no filtering effect at temperatures higher than 100 °C. Massive amounts of the pricy impregnated active carbon is needed to ensure the necessary contact times. Measures like this were not budgeted for and seem unrealistic for a research or industrial project.

The only way to pursue is to reduce the amount of used additive or not use them at all. A dispersion calculation allows to estimate acceptable amounts. The ALOHA (Area Locations of Hazardous Atmospheres) software from the EPA's (Environmental Protection Agency) CAMEO software package is used to evaluate the dispersion calculation. The results are danger zones for the IDHL value (Immediately Dangerous to Life and Health) and the AEGL (Acute Exposure Guideline Levels) and time estimations on how long these zones prolong.

The results showed very high concentrations for short periods of a few minutes. Using a smaller amount of C_6F_6, thus, leading to a reduced additive concentration in the working fluid, will be possible. Neither SO_2 nor $TiCl_4$ are safe enough to use at our test facility. The danger zone (IDHL=100 ppm, AEGL-3=30 ppm) for SO_2 is shown in Figure 15.

Figure 15: results of the dispersion calculation with heavy gas model for a release of 37 kg SO_2 in 3 min with wind direction west, IDHL zone in red, AEGL-3 zone in orange.

DOI: 10.17185/duepublico/77261

OPERATION AND RESULTS – NATIONAL

Our process control system is set up in the software APROL of B&R. Most of our hardware, except the SIL relevant logic components, come from B&R.

Filling CO_2 using a natural circulation cooling system

There are several possible ways to fill a plant or test rig with its working fluid, in this case CO_2. The most obvious one is to use a pump that feeds the working fluid from a storage vessel directly into the system. A process without a pump, only utilizing the pressure difference between the tank and the plant, is possible, but faces the challenge of diminishing pressure differences when both the tank and the system are in a saturated (two-phase) state at the same ambient temperature. Then, both the tank and the plant are at the same saturation pressure and no flow between them can occur. There are two ways to create a (negative) pressure gradient from the tank to the system again:

- Heat the tank, which increases the saturation pressure there
- Cool (at least a part of) the plant, decreasing its pressure

The test rig presented in this paper utilized a natural circulation cooling system that managed to effectively transfer the CO_2 from gas cylinders into the plant without the need of a pump or any other additional equipment. The basic setup is shown in Figure 16:

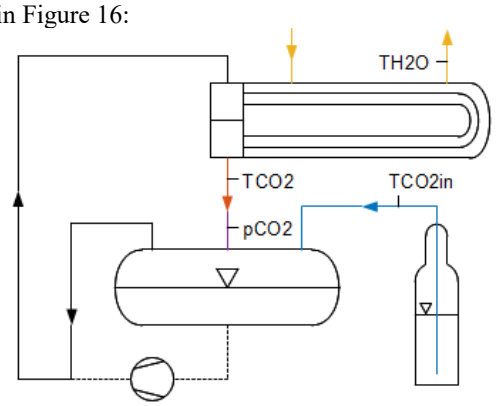

Figure 16: Sketch of the natural circulation cooling system used to fill the test rig with CO_2.

A gas cylinder containing CO_2 in a saturated state is attached to the plant's drum. The gas cylinder has a dip tube to make sure that only the liquid phase is being transferred into the system. CO_2 vapor flows from the drum past the pump (which is shut down) into the plant's cooler (see Figure 2, the heater and expansion valve are omitted in Figure 16). Since the cooling water temperature is about 8 °C and therefore lower than the plant's ambient temperature of about 22 °C in the lab, the CO_2 condenses. Gravity then pulls the liquid CO_2 down into the drum, which creates a void in the cooler that pulls additional gaseous CO_2 into it, resulting in a continuous circulation. Figure 17 demonstrates an actual filling process:

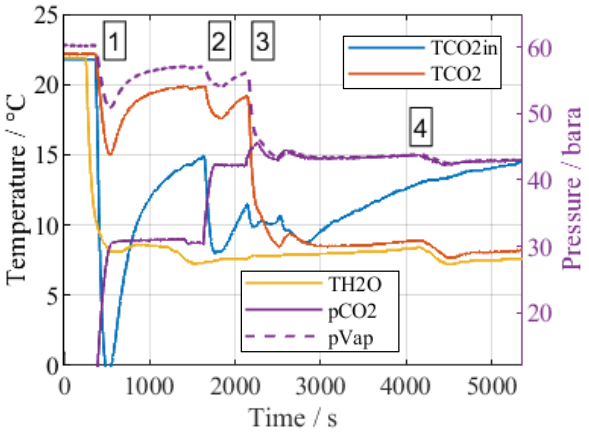

Figure 17: Filling CO_2 using natural circulation cooling.

See Figure 16 for the position of the individual sensors listed in the legend of Figure 17. Before the start of the process, all temperatures (CO_2 inlet temperature *TCO2in*, CO_2 temperature at the outlet of the cooler *TCO2*, cooling water return temperature *TH2O*) are at the ambient temperature of 22 °C and the CO_2 pressure *pCO2* is at 0 barg (the plant is empty). At the time marked with 1, the cooling water valve is opened and cold water at about 8 °C started flowing through the cooler, resulting in a steep decline in the water return temperature. Shortly after, the valve to the first gas cylinder is opened. The expansion of the CO_2 in the gas cylinder into the still empty plant causes a sharp decrease in the CO_2 inlet temperature, which also cooles down the test rig as a whole. The CO_2 pressure increases, but it does not reach the saturation pressure *pVap* yet, which is calculated at the CO_2 temperature *TCO2*. At step 2, another gas cylinder is hooked to the plant, the CO_2 pressure increases further, but the vapor pressure is still not reached. Only after step 3, when two additional (half full) cylinders are attached in short sequence, the CO_2 pressure reaches the vapor pressure, after which both pressures remain practically identical. The fact that the CO_2 vapor is continuously flowing through the cooler and condensing there can be seen at the time marked with 4: the cooling water's two-step temperature controller activates and cooles down the water by a few degrees. The CO_2 temperature followes the water temperature very closely, causing the CO_2 pressure in the plant to decrease. The quick reaction time strongly suggests that CO_2 is flowing through the cooler and natural circulation is established.

DOI: 10.17185/duepublico/77261

Full operation

The process of successful start-up, transcritical operation and shut-down is shown in Figure 18 and Figure 19 with the help of a few parameters. The steps are as follows:

0-1:

- The sCO2 pump is controlled to provide 0.3 kg/s CO_2.
- The electrical heater to heat the thermal oil that will serve as a heat source for the CO_2 is set to manual power. It heats the thermal oil in a primary circuit to 360 °C. With a controlled valve, thermal oil from the secondary circuit is mixed with the primary circuit thermal oil to reach a set temperature of currently 60 °C at $T_{ThOil,ElHeater,Out}$.. By controlling the thermal oil mass flow rate the thermal oil temperature at the inlet of the CO_2 heater is adjusted.
- The water valve controlling the duty at the condenser is opened manually.

1-2:

- The temperature in the tank is controlled by the water flow rate in the condenser. The pressure in the tank/ at the low-pressure side of the test facility remains constant, too.
- This effects back on the thermal oil plant and results in lower temperatures there.

2-8:

- The temperature controller for the thermal oil temperature of the heater´s outlet $T_{ThOil,ElHeater,Out}$ is set to 340 °C and starts ramping up.

3-12:

- The expansion valve controls the pressure on the high-pressure side to 110 bar.
- Pressure oszillations in the pressure on the high-pressure side of the test facility caused by evaporating CO_2 are clearly visible.

4-5:

- The temperature at the outlet of the heater sinks. The controller tries to increase the thermal oil mass flow to reach the temperature $T_{ThOil,CO2Heater,In}$. We will later find out that the thermal oil plant was not properly vented and air was in the system.

6-7:

- The thermal oil mass flow rate breaks down.

8-9:

- The set value for the pressure on the high-pressure side is set to 220 bar. The expansion valve begins to close.

9-10:

- 10 minutes of successful transcritical operation with controlled values.

10-11:

- The expansion valve controller is set to 110 bar.

11-12:

- The coolers in the thermal oil plant cool down the thermal oil temperatures.

12-end:

- The expansion valve is opened and the pressure on the high-pressure side quickly decreases to the low-pressure side level.
- The CO_2 pump and thermal oil pump are turned off.

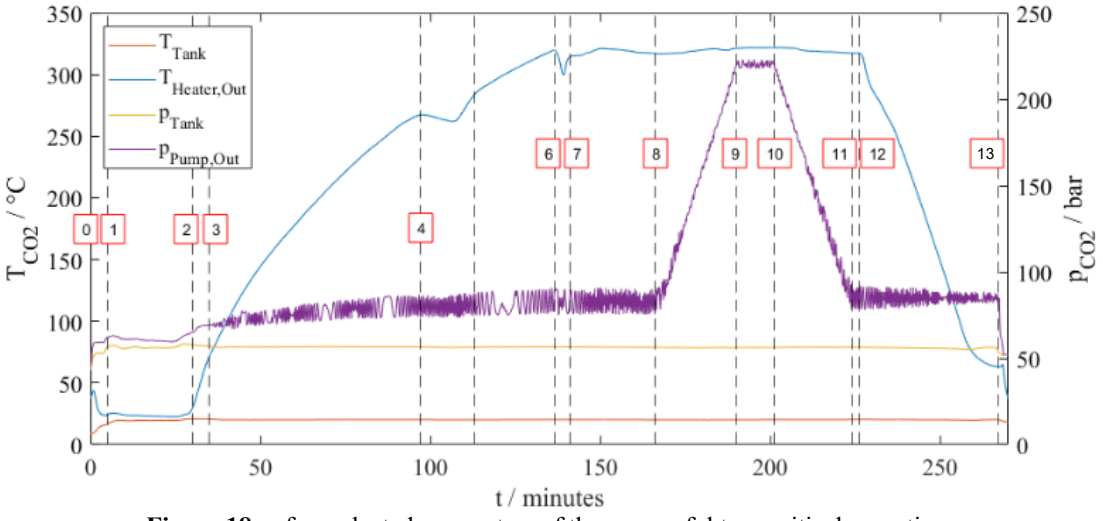

Figure 18: a few selected parameters of the successful transcritical operation.

DOI: 10.17185/duepublico/77261

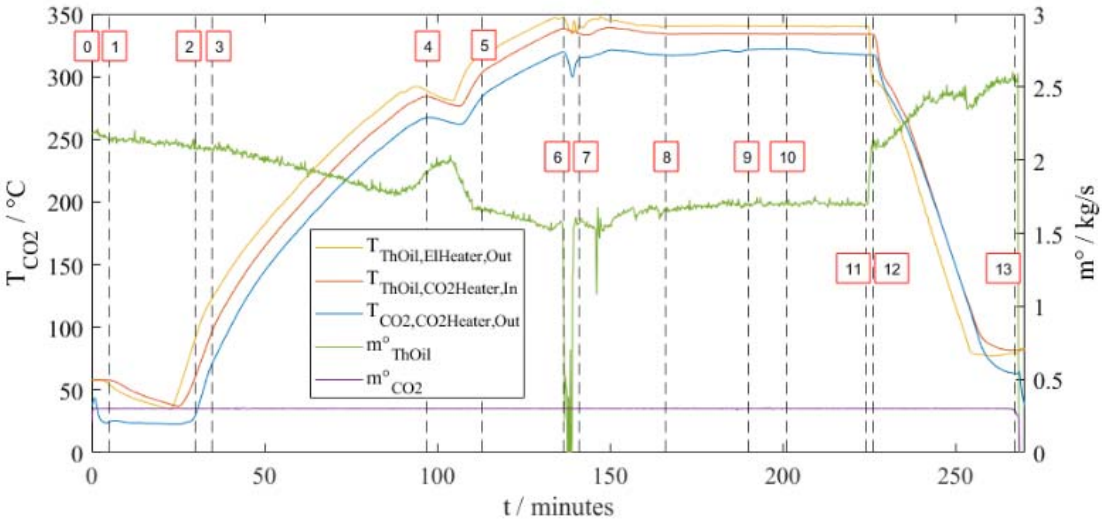

Figure 19: a few selected parameters of the successful transcritical operation.

METHODS AND RESULTS – HEAT TRANSFER

As already mentioned in the design section, some grave mistakes were made during the design phase of the test section. Not-normalized flow into the test section (caused by a lack of an inlet section) caused turbulences so strong that the results in the first half of the test section were completely unusable. In the second half, results were better, but the use of inaccurate measurement equipment led to confidence intervals in the range of several orders of magnitude. This was exacerbated by the fact that small temperature differences had to be measured to accurately determine the heat fluxes, especially when going through the pseudo-critical point, where a spike in the CO_2's specific heat capacity resulted in only minor temperature increases from the inlet to the outlet. CO_2 properties are calculated according to Span and Wagner [45]. A comparison of the results to the predictions when using Gnielinski's correlation [46] is shown in Figure 20:

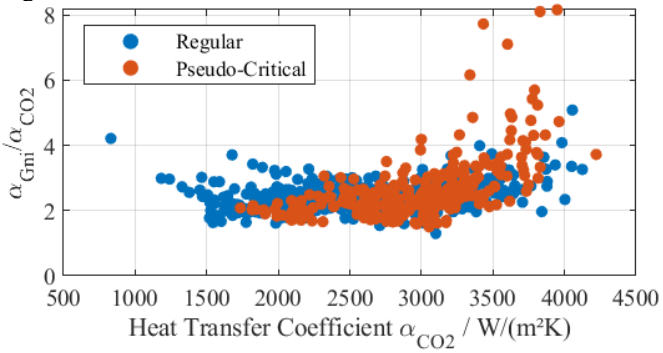

Figure 20: Results of the first test section compared to the predictions when using Gnielinski's correlation.

Figure 20 shows the relative predictions of Gnielinski's correlation to the test section results, categorized in measurements where the CO_2 did not go through the pseudo-critical point (blue points) and those where it did (red points). Results at lower pressures tended to be higher, which is qualitatively correct. One can see that the results were consistently lower than what could be expected from Gnielinski's correlation, most of them by a factor greater than two, and some of the pseudo-critical measurements even going as far as 8 times lower than what could be expected.

LESSONS LEARNED

Measurement equipment and data reduction has to be the first thing to consider.

- Do not compromise here.
- Check with data reduction and error calculation where you could save money. Overly complicated post-processing is avoided and time is saved.
- Plan for over-determined systems to do correction calculations.
- High class temperature sensors are necessary for heat transfer measurements.
- Wall temperature measurement are necessary for heat transfer measurement.
- There is no ideal placement of the Coriolis sensor.
- Use the full potential of Coriolis sensor.
- Use a differential pressure sensor for level measurement, not one using time domain reflectometry.

Collecting data of a certain quality is the heart of experimental research. Besides maybe the side quest of gaining operational experience, creating data is the sole purpose to build an expensive, time-consuming test facility. This is why the measurement system must have priority during the entire project. Saving an insignificant amount of money on a low-quality temperature sensor may not be worth it in the long run.

Performing the data reduction and an error calculation early on might save money at the correct measurement devices. In

DOI: 10.17185/duepublico/77261

other fields, this issue is more prevalent, see for example how experimental physicists deal with it [47].
When there are possibilities to place measurement devices to achieve mathematically over-determined systems, this additional information can be used. A correction calculation according to VDI-guidelines can show inconsistencies in the data, streamline your results and provide smaller error ranges [48].

In the current test facility with a leaking pump, there is no perfect placement for the Coriolis sensor. For future experiments, the position will be changed from the low pressure side before the pump to the high-pressure side after the pump. The sensor will withstand the pressures from a material standpoint but is not recommended to be used by the suppliers. The Coriolis sensor comes with the possibility to simultaneously measure density and temperature. This information can be used to detect gas in the piping where there should be liquid.

Safety measures are necessary and cost intensive.

- Do not only check technical feasibility but speak to suppliers and get a quote.
- Plan for "in-house" preliminary tests tailored to answer project-specific answers.
- Be aware of possible limitations.

See *Safety* in chapter *DESIGN – SCARABEUS* for more information.

A commercial pump with leakage is not suitable for loops.
Per design, the used piston pump does have leakages over the low-to-high pressure sealing and the low-to-ambient pressure sealing which provide cooling exactly where heat from friction is produced. An estimated loss of less than 1‰ might not seem much when the pump is only passed once as it is in its commercial application for filling CO_2 gas cylinders. For the test facility it means losing the inventory over the course of two days.

For future experiments, the leakage from the low-to-high pressure sealing will be collected in a secondary circuit equipped with a cooler to control the pressure. When filled up, it will be pumped back to the main circuit by a second pump. Unfortunately, the second leakage from the low-to-ambient pressure sealing is not collectable.

The pump is not efficient without subcooling.
Maximizing mass flow rate and reducing the amount of leakage are contrary goals. As we use a pump with three pistons, the reached mass flow rate should be linearly correlated to the number of revolutions. Figure 21 shows that the correlation is not linear in comparison to exemplarily shown linear fits of data points at lower numbers of revolutions. The explanation for such behavior is cavitation issues. In the original configuration, the required NPSH value was not reached by far. The state of the CO_2 was too close to the saturated state we have in the tank. The tank is located approx. 1.6 m above the pump. The hydrostatic pressure increase is smaller than for water at a similar temperature range and was not considered accordingly. The by the 1.6 m gained enthalpy difference is probably eaten up by the Coriolis sensor located before the pump.

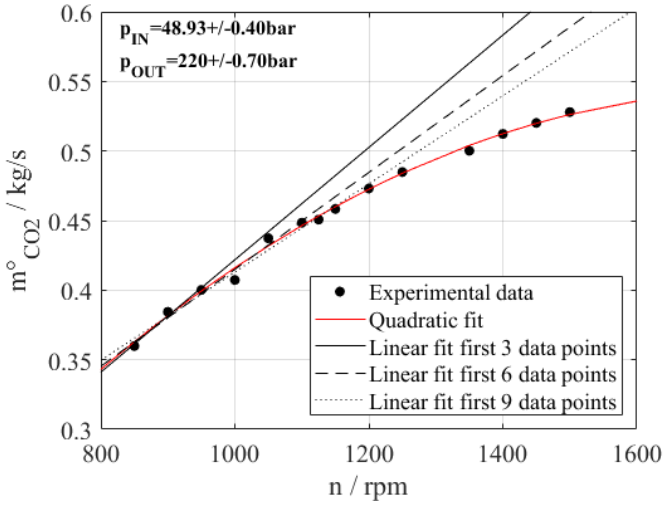

Figure 21: correlation of mass flow rate and number of revolutions.

The following measures were taken to reduce the cavitation issues for the coming SCARABEUS experiments:

- Water cooling of the pump inlet block and pistons.
- Reduced amount of sealing material to reduce the heat brought in by friction.
- Increased allowed number of revolutions from 900 rpm to 1500 rpm in discussion with supplier.
- Subcooling the working fluid by 10 K from saturation conditions before entering the pump in an additional heat exchanger.

CONCLUSION

The sheer size of the original (national) project made it difficult for the small team of scientists to execute it properly within the given time and budget constraints, and lots of mistakes were made because of it. However, the operational experience and lessons learned – in particular the insufficiencies of commercial CO_2 pumps, design of heat transfer measurement equipment and prioritizing measurements and data reduction – have already proved invaluable to the follow-up project SCARABEUS and will continue to serve as the knowledge base for every future project. We failed fast – at least we failed forward.

NOMENCLATURE

Abbreviations

AEGL	Acute Exposure Guideline Levels
BMPC	Bechtel Marine Propulsion Corporation
CFD	Computational Fluid Dynamics
CHNG	China HuaNeng Group
CSIRO	Commonwealth Scientific and Industrial Research Organisation
CSP	Concentrated Solar Power
CVR	Research Center Rez
DOE	U.S. Department of Energy
EDF	Électricité de France

DOI: 10.17185/duepublico/77261

EoS Equation of State
EPA Environmental Protection Agency
GE General Electric
HAZOP Hazard and Operability Study
HT2C High Temperature Heat to Power Conversion facility
IAE Institute of Applied Energy
IDHL Immediately Dangerous to Health and Life
IKE Institut für Kernenergie und Energiesysteme
IST Integrated System Test
iThERM Industrial Thermal Energy Recovery Conversion and Management
KAERI Korean Atomic Energy Research Institute
KAIST Korea Advanced Institute of Science and Technology
KIER Korean Institute of Energy Research
LUT University
Lappeenranta-Lahti University of Technology
NPSH Net Positive Suction Head
SCARABEUS
Supercritical CARbon dioxide/Alternative Blends for Efficiency Upgrade of Solar power plants
SCARLETT
Supercritical CARbon dioxide Loop at IKE Universität StuTTgart
SCIEL Supercritical CO2 Compressor Performance Test Facility
sCO2-HeRO
Supercritical CO2 Heat Removal system
SCO2PE
Supercritical CO2 Pressurising Experiment
SIL Safety and Integrity Level
SNL Sandia National Laboratories
STEP Supercritical Transformational Electric Power Project
SwRI Southwest Research Institute
PCHE Printed Curcuit Heat Exchanger
PHPL Pinjarra Hills High Pressure Test Loop
POSTECH
Pohang University of Science and Technology
RTD Resistance Temperature Detector
TIT Tokyo Institute of Technology
TPRI Xi´an Thermal Power Research Institute

Variables

α_{CO2} heat transfer coefficient as calculated from experimental results ($W/m^2/K$)
α_{Gni} heat transfer coefficient as calculated by Gnielinski´s correlation ($W/m^2/K$)

$\dot{m}_{ThOil}$ mass flow rate of thermal oil (kg/s)
$\dot{m}$, $\dot{m}_{CO2}$ mass flow rate of CO_2 (kg/s)
n revolutions (rpm, revolutions per minute)
p CO_2 pressure (bar)
pCO2 CO_2 pressure in the test facility during filling, measured at the tank (bar), see Figure 14
p_{H2O} water pressure at inlet of test tube (bar), see Figure 6
p_{Tank} CO_2 pressure in the tank (representative for the low-pressure side of the cycle) (bar)
$p_{Pump,Out}$
pVap calculated saturation pressure of CO_2 with TCO2 as input (bar)
P_{IN} CO_2 pressure pump at inlet (bar)
P_{OUT} CO_2 pressure pump at outlet (bar)
p_{thOil} thermal oil pressure (bar)
T_{bulk} CO_2 temperature at the middle of the heat exchanger of the test tube (“bulk temperature”) (°C), see Figure 6
TCO2 CO_2 temperature at the outlet of the water cooler during filling (°C), see Figure 14
$T_{CO2,CO2Heater,Out}$
CO_2 temperature at the outlet of the heater (°C)
TCO2in temperature of CO_2 entering the test facility during filling (°C), see Figure 14
TH2O water temperature at the outlet of the water cooler during filling (°C), see Figure 14
$T_{H2O,in}$ water temperature at the inlet of the test tube (°C), see Figure 6
$T_{H2O,1}$ water temperature at position III of the test tube (°C), see Figure 6
$T_{H2O,2}$ water temperature at position II of the test tube (°C), see Figure 6
$T_{H2O,out}$ water temperature at the outlet of the test tube (°C), see Figure 6
T_{in} CO_2 temperature (°C) at inlet of test section, Figure 5
T_{middle} CO_2 temperature (°C) at the middle of test section, see Figure 5
T_{out} CO_2 temperature (°C) at outlet of test section, Figure 5
T_{Tank} CO_2 temperature in the tank (representative for the low-pressure side of the cycle) (bar)
$T_{Heater,Out}$ CO_2 temperature at the oulet of the heater (°C)
$T_{ThOil,ElHeater,Out}$
thermal oil temperature at the outlet of the electrical heater of the thermal oil plant (°C)
$T_{ThOil,CO2Heater,In}$
thermal oil temperature at the inlet of the CO_2 heater (°C)
$T_{thOil,in}$ thermal oil temperature (°C) at inlet of test section, see Figure 5
$T_{thOil,middle}$
thermal oil temperature (°C) at inlet of test section, see Figure 5
$T_{thOil,out}$ thermal oil temperature (°C) at outlet of test section, see Figure 57
$T_{w,o}$ wall temperature (°C) at outer wall of inner tube of the test tube, see Figure 6, for positions of sensors $T_{w,o1}$, $T_{w,o2}$, and $T_{w,o3}$ see Figure 7
$V°_{H2O}$ volume flow rate of water (l/min)
$V°_{thOil}$ volume flow rate of thermal oil (l/min)

ACKNOWLEDGEMENTS
The authors gratefully thank FFG (Austrian Research Promotion Agency) for funding the current project “CO_2 as a working medium for heat recovery”, Proj. No.: 853568.

DOI: 10.17185/duepublico/77261

The SCARABEUS project has received funding from European Union's Horizon 2020 research program under grant agreement N°814985.

REFERENCES

[1] K. Brun, P. Friedman, and R. Dennis, Eds., *Test facilities*, vol. Fundamentals and Applications of Supercritical Carbon Dioxide (sCO2) Based Power Cycles. Elsevier, 2017. Accessed: Dec. 22, 2022. [Online]. Available: https://linkinghub.elsevier.com/retrieve/pii/B9780081008041000141.

[2] E. M. Clementoni, T. Held, J. Pasch, and J. Moore, "Test facilities," in *Fundamentals and Applications of Supercritical Carbon Dioxide (SCO2) Based Power Cycles*, Elsevier, 2017, pp. 393–414. doi: 10.1016/B978-0-08-100804-1.00014-1.

[3] P. Wu *et al.*, "A review of research and development of supercritical carbon dioxide Brayton cycle technology in nuclear engineering applications," *Nucl. Eng. Des.*, vol. 368, p. 110767, Nov. 2020, doi: 10.1016/j.nucengdes.2020.110767.

[4] M. T. White, G. Bianchi, L. Chai, S. A. Tassou, and A. I. Sayma, "Review of supercritical CO 2 technologies and systems for power generation," *Appl. Therm. Eng.*, vol. 185, p. 116447, Feb. 2021, doi: 10.1016/j.applthermaleng.2020.116447.

[5] A. Yu, W. Su, X. Lin, and N. Zhou, "Recent trends of supercritical CO2 Brayton cycle: Bibliometric analysis and research review," *Nucl. Eng. Technol.*, vol. 53, no. 3, pp. 699–714, Mar. 2021, doi: 10.1016/j.net.2020.08.005.

[6] L. Rapp, "Experimental Testing of a 1MW sCO2 Turbocompressor," presented at the The 7th International Supercritical CO2 Power Cycles Symposium, San Antonio,Texas, Apr. 2019.

[7] M. D. Carlson, "Guidelines for the design and operation of supercritical carbon dioxide R&D systems," presented at the SOLARPACES 2019: International Conference on Concentrating Solar Power and Chemical Energy Systems, Daegu, South Korea, 2020, p. 130003. doi: 10.1063/5.0033262.

[8] E. M. Clementoni and T. L. Cox, "Practical Aspects of supercritical carbon dioxide Brayton system testing," presented at the The 4th International Symposium - Supercritical CO2 Power Cycles, Pittsburgh, Pennsylvania, Sep. 2014.

[9] CSIRO, "Solar-driven Supercritical CO2 Brayton Cycle (1-UFA004) Project results and lessons learnt." May 30, 2017. [Online]. Available: http://www.csiro.au/energy.

[10] A. J. Hacks *et al.*, "Operational experiences and design of the sCO2-HeRo loop," *Conf. Proc. Eur. SCO2 Conf. Eur. Conf. Supercrit. CO2 SCO2 Power Syst. 2019 19th-20th Sept. 2019*, p. 125, Oct. 2019, doi: 10.17185/DUEPUBLICO/48906.

[11] E. Anselmi, V. Pachidis, M. Johnston, I. Bunce, and P. Zachos, "An Overview of the Rolls-Royce sCO2-Test Rig Project at Cranfield University," presented at the The 6th International Supercritical CO2 Power Cycles Symposium, Pittsburgh, Pennsylvania, Mar. 2018.

[12] E. Anselmi, I. Bunce, and V. Pachidis, "An Overview of Initial Operational Experience With the Closed-Loop sCO2 Test Facility at Cranfield University," in *Volume 9: Oil and Gas Applications; Supercritical CO2 Power Cycles; Wind Energy*, Phoenix, Arizona, USA, Jun. 2019, p. V009T38A022. doi: 10.1115/GT2019-91391.

[13] E. Anselmi, P. Belleoud, I. Roumeliotis, and V. Pachidis, "Update of the sCO2-Test Rig at Cranfield University," in *Volume 9: Supercritical CO2*, Rotterdam, Netherlands, Jun. 2022, p. V009T28A024. doi: 10.1115/GT2022-83273.

[14] J. Moore *et al.*, "Commissioning of a 1 MWe Supercritical CO2 Test Loop".

[15] J. J. Moore, M. Day-Towler, J. Mortzheim, S. Cich, and D. Hofer, "TESTING OF A 10 MWe SUPERCRITICAL CO2 TURBINE," 2018.

[16] J. Marion, M. Kutin, A. McClung, J. Mortzheim, and R. Ames, "The STEP 10 MWe sCO2 Pilot Plant Demonstration," in *Volume 9: Oil and Gas Applications; Supercritical CO2 Power Cycles; Wind Energy*, Phoenix, Arizona, USA, Jun. 2019, p. V009T38A031. doi: 10.1115/GT2019-91917.

[17] J. Marion, S. Macadam, A. McClung, and J. Mortzheim, "The STEP 10 MWe sCO2 Pilot Demonstration Status Update," 2022.

[18] J. Marion, "Supercritical CO2, 10 MW Demonstration Project Under Construction," *Glob. J. Energy Equip.*, vol. Turbomachinery International, no. Vol 63, 5, Oct. 2022.

[19] S. Martin *et al.*, "Progress Update on the Allam Cycle: Commercialization of Net Power and the Net Power Demonstration Facility," *SSRN Electron. J.*, 2019, doi: 10.2139/ssrn.3366370.

[20] NET Power, "First Utility-Scale Project," Dec. 2022. https://netpower.com/first-utility-scale-project/.

[21] J. E. Cha, S. W. Bae, J. Lee, S. K. Cho, J. I. Lee, and J. H. Park, "Operation Results of a Closed Supercritical CO2 Simple Brayton Cycle," 2016.

[22] S. J. Bae, Y. Ahn, J. Lee, S. G. Kim, S. Baik, and J. I. Lee, "Experimental and numerical investigation of supercritical CO 2 test loop transient behavior near the critical point operation," *Appl. Therm. Eng.*, vol. 99, pp. 572–582, Apr. 2016, doi: 10.1016/j.applthermaleng.2016.01.075.

[23] J. Lee, S. Baik, S. K. Cho, J. E. Cha, and J. I. Lee, "Issues in performance measurement of CO2 compressor near the critical point," *Appl. Therm. Eng.*, vol. 94, pp. 111–121, Feb. 2016, doi: 10.1016/j.applthermaleng.2015.10.063.

[24] J. Cho *et al.*, "Development of the Supercritical Carbon Dioxide Power Cycle Experimental Loop in KIER," in *Volume 9: Oil and Gas Applications; Supercritical CO2 Power Cycles; Wind Energy*, Seoul, South Korea, Jun. 2016, p. V009T36A013. doi: 10.1115/GT2016-57460.

[25] B. Choi *et al.*, "Development of a 500 °C semi-pilot scale supercritical CO2 power cycle test loop," presented at the

SOLARPACES 2020: 26th International Conference on Concentrating Solar Power and Chemical Energy Systems, Freiburg, Germany, 2022, p. 090003. doi: 10.1063/5.0085681.

[26] M. Aritomi, T. Ishizuka, Y. Muto, and N. Tsuzuki, "Performance Test Results of a Supercritical CO2 Compressor Used in a New Gas Turbine Generating System," *J. Power Energy Syst.*, vol. 5, no. 1, pp. 45–59, 2011, doi: 10.1299/jpes.5.45.

[27] Y. Le Moullec *et al.*, "Shouhang-EDF 10MWe supercritical CO2 cycle + CSP demonstration project," *Conf. Proc. Eur. SCO2 Conf. Eur. Conf. Supercrit. CO2 SCO2 Power Syst. 2019 19th-20th Sept. 2019*, p. 138, Oct. 2019, doi: 10.17185/DUEPUBLICO/48884.

[28] H. Li, Y. Zhang, M. Yao, Y. Yang, W. Han, and W. Bai, "Design assessment of a 5 MW fossil-fired supercritical CO2 power cycle pilot loop," *Energy*, vol. 174, pp. 792–804, May 2019, doi: 10.1016/j.energy.2019.02.178.

[29] L. Seshadri *et al.*, "Design of 20 kW Turbomachinery for Closed Loop Supercritical Carbon Dioxide Brayton Test Loop Facility," in *Volume 9: Oil and Gas Applications; Supercritical CO2 Power Cycles; Wind Energy*, Phoenix, Arizona, USA, Jun. 2019, p. V009T38A016. doi: 10.1115/GT2019-90876.

[30] B. Twomey *et al.*, "The University of Queensland Refrigerant and Supercritical CO2 Test Loop," in *Volume 3: Coal, Biomass and Alternative Fuels; Cycle Innovations; Electric Power; Industrial and Cogeneration; Organic Rankine Cycle Power Systems*, Seoul, South Korea, Jun. 2016, p. V003T25A013. doi: 10.1115/GT2016-58110.

[31] "ASTRI Australian Solar Thermal Research Institute," ASTRI, Public Dissemination Report, Jun. 2019. Accessed: Dec. 22, 2022. [Online]. Available: https://www.astri.org.au/publications/reports/.

[32] "AUSTRALIAN SOLAR THERMAL RESEARCH INSTITUTE (ASTRI)," ASTRI, Public Dissemination Report, 2021. Accessed: Dec. 22, 2022. [Online]. Available: https://www.astri.org.au/publications/reports/.

[33] L. Toni, G. Persico, P. di Milano, E. F. Bellobuono, R. Valente, and P. Gaetani, "Experimental and Numerical Performance Survey of a MW-Scale Supercritical CO2 Compressor Operating in Near-Critical Conditions".

[34] P. Hajek and O. Frybort, "EXPERIMENTAL LOOP S-CO2 SUSEN".

[35] A. Vojacek, V. Dostal, F. Goettelt, M. Rohde, and T. Melichar, "Performance Test of the Air-Cooled Finned-Tube Supercritical CO2 Sink Heat Exchanger," *J. Therm. Sci. Eng. Appl.*, vol. 11, no. 3, p. 031014, Jun. 2019, doi: 10.1115/1.4041686.

[36] W. Flaig, R. Mertz, and J. Starflinger, "Setup of the Supercritical CO2 Test Facility 'SCARLETT' for Basic Experimental Investigations of a Compact Heat Exchanger for an Innovative Decay Heat Removal System," *J. Nucl. Eng. Radiat. Sci.*, vol. 4, no. 3, p. 031004, Jul. 2018, doi: 10.1115/1.4039595.

[37] "Data of simple CO2 experiment for code validation," DELIVERABLE NO. 2.1, 2017.

[38] S. Schuster, A. Hacks, and D. Brillert, "Lessons from testing the sCO2-HeRo turbo-compressor-system".

[39] G. Bianchi *et al.*, "Design of a high-temperature heat to power conversion facility for testing supercritical CO2 equipment and packaged power units," *Energy Procedia*, vol. 161, pp. 421–428, Mar. 2019, doi: 10.1016/j.egypro.2019.02.109.

[40] G. Petruccelli, A. Uusitalo, A. Grönman, T. Turunen-Saaresti, and M. Zocca, "CLOSED-LOOP SUPERCRITICAL CARBON DIOXIDE WIND TUNNEL: DESIGN AND COMPONENTS," presented at the The 4th European sCO2 Conference for Energy Systems, Online, Mar. 2021.

[41] R. C. Hendricks, R. J. Simoneau, and R. V. Smith, "Survey of Heat Transfer to Near-Critical Fluids," National Aeronautics and Space Administration Washington, D. C., NASA TN D-5886, Technical Note, 1970.

[42] V. Illyés *et al.*, "Design of an Air-Cooled Condenser for CO2-Based Mixtures: Model Development, Validation and Heat Exchange Gain with Internal Microfins," in *Volume 9: Supercritical CO2*, Rotterdam, Netherlands, Jun. 2022, p. V009T28A016. doi: 10.1115/GT2022-82438.

[43] G. Di Marcoberardino *et al.*, "Experimental characterisation of CO2 + C6F6 mixture: Thermal stability and vapour liquid equilibrium test for its application in transcritical power cycle," *Appl. Therm. Eng.*, vol. 212, p. 118520, Jul. 2022, doi: 10.1016/j.applthermaleng.2022.118520.

[44] P.-L. David, "Public report on the heat transfer characteristics using CO2 blends," D4.3 Public report, 2021. [Online]. Available: https://www.scarabeusproject.eu/2021/07/10/d4-3-public-report-on-the-heat-transfer-characteristics-using-co2-blends/

[45] R. Span and W. Wagner, "A New Equation of State for Carbon Dioxide Covering the Fluid Region from the Triple-Point Temperature to 1100 K at Pressures up to 800 MPa," *J. Phys. Chem. Ref. Data*, 1996, doi: https://doi.org/10.1063/1.555991.

[46] V. Gnielinski, "G1 Heat Transfer in Pipe Flow. In: VDI Heat Atlas," Berlin, Heidelberg: Springer, 2010. [Online]. Available: https://doi.org/10.1007/978-3-540-77877-6_34

[47] M. Drosg, *Dealing with Uncertainties : a Guide to Error Analysis*, 2., Enlarged edition. Berlin: Springer, 2009.

[48] Verein Deutscher Ingenieure e.V., Ed., "Kontrolle und Verbesserung der Qualität von Prozessdaten und deren Unsicherheiten mittels Ausgleichsrechnung bei Betriebs- und Abnahmemessungen (Control and quality improvement of process data and their unvertainties by means of correction calculation for operation and acceptance tests)." Beuth Verlag GmbH, Berlin.

DOI: 10.17185/duepublico/77261

ANNEX A

DETAILS ON EQUIPMENT

Component	Manufacturer	Detail
Heater	Funke	200 kW, Shell-and-Tube, CO_2 tube-side, thermal oil VP-1 shell-side
Cooler/ condenser	Funke	355 kW, Shell-and-Tube, CO_2 tube-side, water shell-side
Pump	Speck Triplex Pumpen	Piston-pump (SPECK-TRIPLEX-PLUNGERPUMPE P52/51-300CZ), max. 50 L/min, Pmax=180 bar
Expansion valve	Samson	Pneumatic control valve, type 3252
Tank	Reisenauer	55 L

Measurement equipment	Type	Manufacturer
Temperature	PT100 class AA, A, B	Wika, Endress+Hauser,
Pressure		ICCP Messtechnik GmbH
Mass flow, density	Coriolis	Endress+Hauser
Level (1st try)	Time Domain Reflectometry	Endress+Hauser
Level (2nd try)	Differential pressure	Endress+Hauser

DOI: 10.17185/duepublico/77261

DOI: 10.17185/duepublico/77261
URN: urn:nbn:de:hbz:465-20230427-101011-6